Eur. Phys. J. D **43**, 169–172 (2007)
DOI: 10.1140/epjd/e2007-00077-9

THE EUROPEAN PHYSICAL JOURNAL D

Noble gas and metal clusters in carbon nanopores: from models to applications

N.V. Krainyukova[a] and V.G. Belan

Institute for Low Temperature Physics and Engineering NASU, 47 Lenin ave., Kharkov 61103, Ukraine

Received 23 July 2006 / Received in final form 29 September 2006
Published online 24 May 2007 –

Abstract. Low temperature high energy (50 keV) electron diffraction experiments are performed in the both transmission and reflection regimes to study noble gas as well as aluminium clusters formed in nanoporous confinement of 'amorphous' carbon films. Results are compared with calculations made for multiply twined particles such as icosahedra (ico) and decahedra (dec) with five-fold symmetry as well as face-centred cubic and hexagonal close-packed clusters. The analysis was based on the comparison of precise experimental and calculated diffracted intensities with the help of the R (reliability) — factor minimization with respect to relative weights w_N of model-clusters of different sizes N(numbers of atoms) considered as variables in this procedure. The highly reproducible discrete distribution functions of sizes and structures characterize the suggested method as a good application to a pore medium description. The temperature related effects in the deposition processes as well as the specific growth mechanisms were revealed and discussed.

PACS. 61.46.-w Nanoscale materials – 61.14.-x Electron diffraction and scattering – 36.40.-c Atomic and molecular clusters – 81.05.Rm Porous materials; granular materials

1 Introduction

Multiply twined particles (MPTs) [1–5] first discovered in sixties of last century nowadays play an increasing role in nanoscience and numerous applications. Their appearance owes to the minimum surface energy realised in these particles as compared with single crystal clusters. The surface energy competes with the deformation energy arising due to five-fold symmetry axes that result in a failure of MTPs at growing sizes. Numerous facts of MTP's observations were reported. They were found in gas expansion experiments [5–17], in growth processes on substrate at relatively high super saturations [1,2], they are expected in abundances of particles formed by impurity injecting into superfluid helium [18–20] as well as in clusters grown inside of nanoporous materials [21–30].

Nanostructured carbon-based materials, whose carbon sheet curvatures and structural arrangements range from nanometers up to several hundred nanometers, represent a class of solids with a variety of drastically different properties. So-called schwartzites [31,32] formed by negatively curved graphitic sheets are permitted by interconnected channels and can be considered as a kind of porous matrix, which may be filled with different substances under certain conditions.

[a] e-mail: krainyukova@ilt.kharkov.ua

2 Experimental details and the analysis method

Low temperature high energy (50 keV) electron diffraction study of films formed by so-called 'amorphous' [32] carbon (with micro- and mesopores accordingly to the classification [31]) filled with solidified noble gases as well as with aluminium is presented. The neon and argon preparation procedure was described in details previously [28–30]; briefly gases were deposited on substrate (evacuated from backside) inside of the electron diffraction set-up at low temperatures. Aluminium samples were prepared in a similar way by the metal sublimation in vacuum and studied at room temperatures. Porous carbon films were produced from vacuum sublimated graphite (by the electric current heating of thin carbon rods of approximately 1 mm or thinner in diameters, the arc discharge was avoided) with deposition onto two types of the salt (NaCl) sublayers. One was the cleaved single crystal (SC) surface while the other was the polycrystalline (PC) salt films prepared by the sublimation in vacuum. Both substrates were solved in water; carbon films were put onto the copper net (with a high thermal conductivity and transparent for electrons) by means of the floating of carbon films. Prepared in such ways carbon films were evacuated during several hours before gas and aluminium deposition. Argon gas of a room temperature was deposited inside the helium cryostat while neon was precooled to a liquid

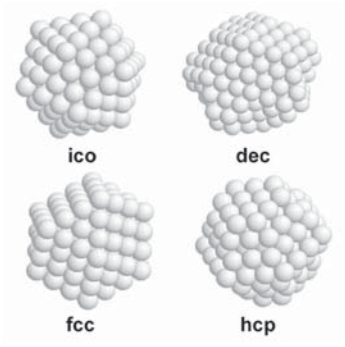

Fig. 1. Examples of model-clusters used in the applied simulations of diffraction patterns: icosahedra (ico), decahedra (dec), fcc and hcp clusters.

nitrogen temperature before deposition. Both gas samples were studied at 6 K. Aluminium samples were prepared and investigated at room temperatures. We applied two electron diffraction regimes: the transmission and the reflection. In the later regime we used grazing electrons reflected from the backside of films, i.e. not exposed by the deposited atoms during preparation. The effective thickness δ of deposits characterised the total amount of condensed materials and the pore filling. All diffraction data were collected in the form of numerical files.

Diffractograms were analysed by means of the applied simulations, which were made in the similar way as it was described previously [28–30], i.e. on the basis of an assumption of a wide enough variety of possible involved structures and sizes in the observed composition of formed clusters. Together with single cluster formations such as cuboctahedra and hcp clusters we included in our analysis MTPs with five-fold symmetry, i.e. non-crystallographic multishell icosahedra (ico) [33] and Mark's decahedra (dec) [34], with initially from one up to 20 shells for every structural type (for the examples see Fig. 1). The diffracted intensity (per atom) for each cluster k comprising N_k atoms was calculated using Debye formulae

$$I_{\mathrm{calc},k}(s) = (f^2 + s^{-4}S(s))/(1-t) + 2f^2 N_k^{-1} \exp(-\langle u^2\rangle_k s^2)(\Sigma(\sin sr_{ij})/(sr_{ij}))_k;$$

here the fraction t of atoms is assumed to be free (i.e. not bonded to the cluster). The summation in the interference function runs in the cluster k over all pairs of atoms $i > j$, separated by the distance r_{ij}; the Debye-Waller factor $\exp(-\langle u^2\rangle_k s^2)$ allows for mean-square atomic displacements $\langle u^2\rangle_k$, $f(s)$ is the elastic atomic scattering factor for electrons, $S(s)$ is the incoherent X-ray scattering factor. The superposition of diffracted intensities I_{calc} from different clusters k with their relative weights w_k, i.e. $I_{\mathrm{calc}} = \Sigma w_k I_{\mathrm{calc},k}$, was compared with experimental intensities I_{exp} using the reliability factor R in the form $R = \Sigma|I_{\mathrm{exp}} - I_{\mathrm{calc}}|/\Sigma(I_{\mathrm{exp}} + I_{\mathrm{calc}})$, where the summation was taken over approximately 300–400 points along the experimental and calculated diffraction patterns with the equidistant step $\sim$0.015 Å^{-1} in $s = 4\pi\sin(\theta)/\lambda$ (θ is the diffraction angle and λ is the wavelength of electrons). The values w_k were involved in the total analysis as nearly independent variables [28–30]. The total Σw_k of all relative weights is equal to 1.

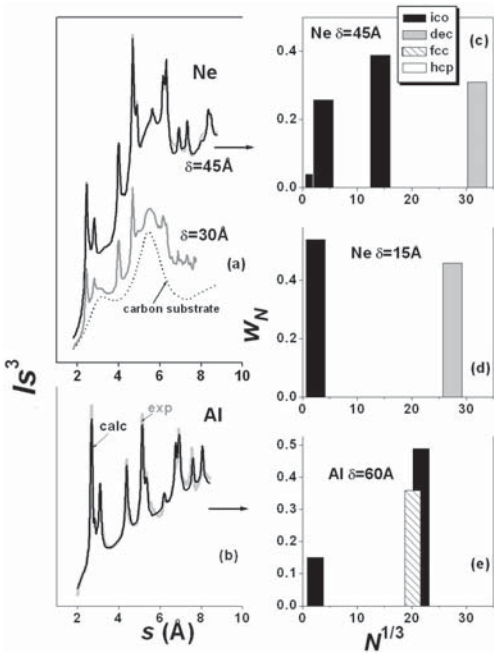

Fig. 2. Experimental (grey) and calculated (black) diffractograms for Ne (δ = 30 Å and δ = 45 Å) (a) and Al (δ = 60 Å) (b) samples deposited on carbon films *prepared on the single crystal salt sublayer*. In the case of the Al sample the substrate contribution (a, the dot line) is subtracted. The distribution functions of Ne clusters over sizes and structures for δ = 45 Å (c), δ = 15 Å (d) and Al clusters with δ = 60 Å (e). The inset shows the structure identifications.

3 Neon and aluminium clusters in 'amorphous' carbon

Noble gas clusters formed in nanopores of 'amorphous' carbon were studied previously [28–30]. We revealed several general tendencies, which should be mentioned in view of their anticipated and confirmed in this work applicability to the wide group of objects including metals. We have found earlier [30] that $T = 0.25T_{\mathrm{m}}$ is the boundary temperature (T_{m} is the melting temperature); above this point small clusters with $N \sim$ 13–55 atoms form while below the smallest clusters were of several hundred atoms in a size. Experiments performed on Al confirmed that smallest clusters with $N \sim$ 13–55 atoms form in the case of metals at the same relative preparation temperatures, which is close to $\sim 0.3T_{\mathrm{m}}$ for Al at $T \sim$ 300 K.

In Figure 2 we show typical experimental and calculated diffractograms for Ne and Al samples prepared at 6 and 300 K respectively by deposition on carbon films prepared on the SC salt sublayer. Applying the method described in the previous section we obtained the size and structure distribution functions (Figs. 2c–2e). These distributions demonstrate the absolute dominance (65–100%) of ico and dec clusters with five-fold symmetry. Moreover these clusters appear in the size intervals predicted in the theory made for free clusters [35], i.e. ico for sizes below $N \sim$ 3000 atoms while dec were found for larger sizes. Smaller fractions of the fcc were ascribed [30]

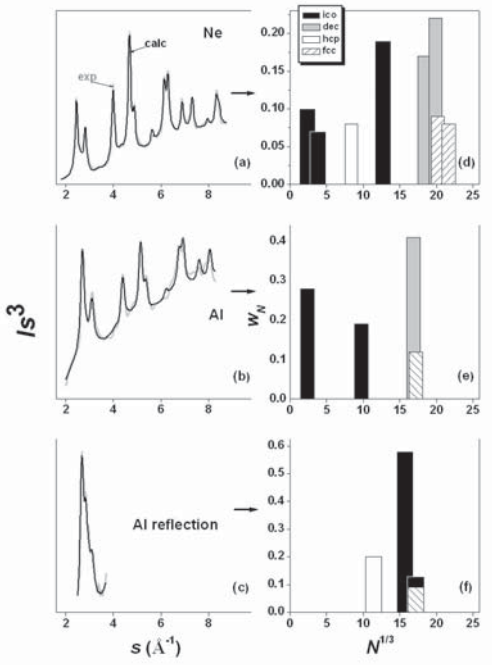

Fig. 3. Experimental (grey) and calculated (black) diffractograms for Ne ($\delta = 55$ Å) (a) and Al ($\delta = 40$ Å) (b) samples. Diffraction patterns are recorded in transmission (a, b) and reflection (c, Al with $\delta = 200$ Å) regimes. The samples are grown on carbon films *prepared on the polycrystalline salt sublayer*. The substrate contribution is subtracted. The relevant distribution functions are shown on the left.

to the minor differences between fcc and dec for cluster sizes N about several thousand atoms and to the incomplete growth.

At the earlier growth stage we observed only two types of sizes, i.e. smallest and largest ones (Fig. 2d). Absence of intermediate sizes in this stage, which appear at the higher film filling (Fig. 2c), we ascribe to the fact that large defects form *inside* films because otherwise all sizes should be 'visible' at the beginning. We conclude that the substance directly deposited on substrate in the form of large clusters later penetrate in smaller pores due to the diffusive-like processes [30,36] at high enough temperatures. Pores closest to the surface are filled first, while the deeper ones later. Thus, largest clusters form in the essentially open geometry that makes it possible to use widely these so-called 'amorphous' carbon films in the electron microscopy and the electron diffraction as supporting substrates mainly due to the absence of distinct diffraction peaks from such films intersecting with lines of studied materials deposited upon substrates. But it was shown [32] and confirmed in our previous studies [28–30] that carbon films prepared by means of vacuum sublimation of graphite also exhibit several important features, which characterize them as a porous matrix with very fine channels.

Applying carbon films deposited on polycrystalline salt sublayer we obtained diffraction patterns from neon and aluminium samples (Fig. 3) by means of two electron diffraction regimes, i.e. transmission and reflection. The relevant distribution functions are shown on the left in Figure 3. For this type of carbon substrates we also revealed the prevalence of MTPs. Microsized ($N <$ 60 atoms) clusters are mixed with mesosized species (N on an order of magnitude stretches from several hundred to several thousand atoms, for the classification see [31]) with the noticeable gap between smallest clusters and $N \sim$ 700–1000 atoms. The population of clusters with intermediate sizes is noticeably higher in this case, i.e. on the carbon substrate prepared on a polycrystalline salt sublayer as compared with single crystal salt, evidently because of a larger amount of defects formed inside carbon films. Diffraction experiments performed in the reflection regime from the backside of filled carbon films (Fig. 3c), i.e. not exposed by the deposited atoms during preparation, revealed distinct first Al peaks that confirmed the deep penetration of metal atoms into the porous substrate. In this case we see only the mesosized clusters apparently due to the hindered deeper diffusion to smallest pores.

Accordingly to our estimations based on numerous experimental materials (and for different objects) the part t of deposits, which is not bonded to clusters, can reach in some deposits more than 50% the total amount of deposited substance and is nearly independent on some intermediate effective thickness of condensed materials. At first sight we could ascribe this feature to the Stranski-Krastanov growth scheme [37] because at higher temperatures (above $\sim$0.35 $T_{\rm m}$) we observed the similar time delay (as described long ago by Venables [38]) between the deposition beginning and the distinct peaks appearance. This scheme assumes the intermediate layer formation between clusters and substrates before the cluster growth because of much stronger interaction between deposited atoms and substrate than between condensed atoms themselves. Previously we have found [36] the essentially damped atomic dynamics in neon clusters formed in pores ascribed to stronger interaction of neon atoms with carbon walls. Distinct diffraction peaks can be produced only by clusters described by the second oscillating term in the formula given above while atoms not bonded to clusters form only the contribution to the first monotonic term. But in contrast with expectations at lower deposition temperatures no time delay was observed, moreover at first growth stages distinct cluster peaks were successfully described by the formulae with $t = 0$. In other words we see the zero contribution of atoms not bonded to clusters at earlier growth stages, i.e. clusters grow first. We could ascribe this feature simply to the reduced wetting due to the strong interaction with substrates [39,40]. But t rapidly grows up to several dozens percents with the growing deposit portions (Fig. 4). This observation implies also that smaller voids form inside porous matrix and are filled at the later growth stages with deposited atoms diffusively or due to capillary processes because potential barriers delay penetration into these positions at earlier stages. In addition we can emphasize also the possible role of the 'effective pressure' arising in larger pores and 'pushing' atoms in the smaller ones.

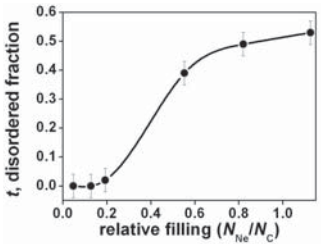

Fig. 4. Dependence of the disordered fraction t of Ne samples on the filling of carbon films prepared on the single crystal salt sublayer.

4 Conclusions

In line with our previous observations [28–30] this work confirms that clusters formed in porous carbon films are self-selected in sizes that is presumably induced by the discrete character of micro- and mesosizes of pores [31]. We have also found in this work that carbon films formed by means of the deposition on polycrytalline and single crystal salt sublayers are essentially different in porous substructures reduced from suggested analysis; mesopores preferably form in carbon films under the deposition upon a polycrystalline salt sublayers (apparently due to their initial surface roughness) in contrast with smooth single crystal salt surfaces.

Size and structure distribution functions exhibit for all objects under study absolute prevalence of MTPs, i.e. clusters with five-fold symmetry axes. The formation of smallest clusters (with sizes ∼13–55 atoms) were confirmed to be affected by the preparation temperature, i.e. such clusters grow at temperatures above $\sim 0.25 T_{\rm m}$. This observation was generalised in this work in an application to aluminium clusters. We explain this effect by thermally activated processes that make it possible to fill smallest pores due to diffusion. Our work does not encourage the Stranski-Krastanov growth scheme in application to the porous carbon substrate. The crystalline phase appears first in the form of clusters, then smaller clusters grow inside substrate due to diffusion and capillary processes and at last the disordered component appears at latter growth stages filling the smallest voids inside substrate in positions, where no crystalline phase can exist.

The authors are grateful to V.G. Manzhelii, M.A. Strzhemechny, V. Khmelenko, V. Kiryukhin and A.I. Prokhvatilov for valuable comments; they are also greatly indebted to B.W. van de Waal for fruitful discussions and also for software, which was applied to cluster modelings.

References

1. H. Hofmeister, in *Encyclopedia of Nanoscience and Nanotechnology*, edited by H.S. Nalwa (American Scientific Publishers, Los Angeles, 2004), V. 3, pp. 431–452
2. L.D. Marks, Rep. Prog. Phys. **57**, 603 (1994)
3. B. Raoult, J. Farges, M.F. De Feraudy, G. Torchet, Phil. Mag. B **60**, 881 (1989)
4. T.P. Martin, Phys. Rep. **273**, 199 (1996)
5. B.W. van de Waal, *The FCC/HCP Dilemma* (B.V. Febodruk, Enschede, 1997)
6. J. Farges, M.F. de Feraudy, B. Raoult, G. Torchet, J. Chem. Phys. **78**, 5067 (1983)
7. J. Farges, M.F. de Feraudy, B. Raoult, G. Torchet, J. Chem. Phys. **84**, 3491 (1986)
8. B.W. van de Waal, G. Torchet, M.-F. de Feraudy, Chem. Phys. Lett. **331**, 57 (2000)
9. M.-F. de Feraudy, G. Torchet, J. Cryst. Growth **217**, 449 (2000)
10. B.W. van de Waal, J. Chem. Phys. **98**, 4909 (1993)
11. T. Ikeshoji, G. Torchet, M.-F. de Feraudy, K. Koga, Phys. Rev. E **63**, 031101 (2001)
12. O.G. Danylchenko, S.I. Kovalenko, V.N. Samovarov, Fiz. Nizk. Temp. **30**, 986 (2004) [Low Temp. Phys. **30**, 743 (2004)]
13. O.G. Danylchenko, S.I. Kovalenko, V.N. Samovarov, Fiz. Nizk. Temp. **30**, 226 (2004) [Low Temp. Phys. **30**, 166 (2004)]
14. S.I. Kovalenko, D.D. Solnyshkin, E.T. Verkhovtseva, V.V. Eremenko, Chem. Phys. Lett. **250**, 309 (1996)
15. D. Reinhard, B.D. Hall, P. Berthoud, S. Valkealahti, R. Monot, Phys. Rev. Lett. **79**, 1459 (1997)
16. D. Reinhard, B.D. Hall, D. Ugarte, R. Monot, Phys. Rev. B **55**, 7868 (1997)
17. D. Reinhard, B.D. Hall, P. Berthoud, S. Valkealahti, R. Monot, Phys. Rev. B **58**, 4917 (1998)
18. V. Kiryukhin, B. Keimer, R.E. Boltnev, V.V. Khmelenko, E.B. Gordon, Phys. Rev. Lett. **79**, 1774 (1997)
19. S.I. Kiselev, V.V. Khmelenko, D.M. Lee, V. Kiryukhin, R.E. Boltnev, E.B. Gordon, B. Keimer, Phys. Rev. B **65**, 024517 (2001)
20. E.P. Bernard, R.E. Boltnev, V.V. Khmelenko, V. Kiryukhin, S.I. Kiselev, D.M. Lee, Phys. Rev. B **69**, 104201 (2004)
21. D.W. Brown, P.E. Sokol, S.N. Ehrlich, Phys. Rev. Lett. **81**, 1019 (1998)
22. T. Hofmann, D. Wallacher, P. Huber, K. Knorr, J. Low Temp. Phys. **140**, 91 (2005)
23. P. Huber, K. Knorr, Phys. Rev. B **60**, 12657 (1999)
24. M.P. Fang, P.E. Sokol, Phys. Rev. B **52**, 12614 (1995)
25. B. Schäfer, D. Balszunat, W. Langel, B. Asmussen, Mol. Phys. **89** (1996) 1057
26. D. Wallacher, P. Huber, K. Knorr, J. Low Temp. Phys. **122**, 313 (2001)
27. D.E. Silva, P.E. Sokol, S.N. Ehrlich, Phys. Rev. Lett. **88**, 155701 (2002)
28. N.V. Krainyukova, B.W. van de Waal, Thin Solid Films **459**, 169 (2004)
29. N.V. Krainyukova, Surf. Interf. Anal. **38**, 469 (2006)
30. N.V. Krainyukova, Thin Solid Films **515**, 2792 (2006)
31. E. Barborini, P. Piseri, P. Milani, G. Benedek, C. Ducati, J. Robertson, Appl. Phys. Lett. **81**, 3359 (2002)
32. S.J. Townsend, T.J. Lenosky, D.A. Muller, C.S. Nickols, V. Elser, Phys. Rev. Lett. **69**, 921 (1992)
33. A.L. Mackay, Acta Cryst. **15**, 916 (1962)
34. L.D. Marks, Phil. Mag. A **49**, 81 (1984)
35. N.V. Krainyukova, Thin Solid Films **515**, 1658 (2006)
36. N.V. Krainyukova, AIP Proceedings **850**, 390 (2006) (the 24th International Conference on Low Temperature Physics, Orlando, Florida, August 10–17, 2005)
37. J.A. Venables, G.D.T. Spiller, M. Hanbücken, Rep. Progr. Phys. **47**, 399 (1984)
38. J.A. Venables, D.J. Ball, Proc. Roy. Soc. Lond A **322**, 331 (1971)
39. A. Esztermann, M. Heni, H. Löwen, J. Klier, M. Sohaili, P. Leiderer, Phys. Rev. Lett. **88**, 055702 (2002)
40. F.T. Gittes, M. Schick, Phys. Rev. B **30**, 209 (1984)